AD-A039 181   CIVIL ENGINEERING LAB (NAVY) PORT HUENEME CALIF.   F/G 20/3
                 TECHNIQUES FOR TRANSFER IMMITTANCE MEASUREMENTS.(U)
                 MAR 77   K T HUANG, D M SHIROMA
UNCLASSIFIED   CEL-TN-1473   NL

| OF |
ADA039181

END
DATE
FILMED
5-77

Technical Note

CEL

TN no. N-1473

title: TECHNIQUES FOR TRANSFER IMMITANCE MEASUREMENTS

author: K. T. Huang, Ph.D. and D. M. Shiroma

date: March 1977

sponsor: CHIEF OF NAVAL MATERIAL

program nos: Z-R000-01-142

D D C
MAY 9
C

CIVIL ENGINEERING LABORATORY

NAVAL CONSTRUCTION BATTALION CENTER
Port Hueneme, California 93043

REPORT DOCUMENTATION PAGE		READ INSTRUCTIONS BEFORE COMPLETING FORM
1. REPORT NUMBER CEL – TN-1473	2. GOVT ACCESSION NO DN587002	3. RECIPIENT'S CATALOG NUMBER
4. TITLE (and Subtitle) TECHNIQUES FOR TRANSFER IMMITTANCE MEASUREMENTS		5. TYPE OF REPORT & PERIOD COVERED Not final; Jul 1974 – Aug 1976
		6. PERFORMING ORG. REPORT NUMBER
7. AUTHOR(s) K. T. Huang, Ph.D., D. M. Shiroma		8. CONTRACT OR GRANT NUMBER(s) ZR000 01 142
9. PERFORMING ORGANIZATION NAME AND ADDRESS CIVIL ENGINEERING LABORATORY Naval Construction Battalion Center Port Hueneme, California 93043		10. PROGRAM ELEMENT, PROJECT, TASK AREA & WORK UNIT NUMBERS 61152N; Z R000 01-142
11. CONTROLLING OFFICE NAME AND ADDRESS Chief of Naval Material, Navy Department Washington, D. C. 20360		12. REPORT DATE Mar 1977
		13. NUMBER OF PAGES 33
14. MONITORING AGENCY NAME & ADDRESS(if different from Controlling Office)		15. SECURITY CLASS. (of this report) Unclassified
		15a. DECLASSIFICATION DOWNGRADING SCHEDULE

16. DISTRIBUTION STATEMENT (of this Report)

Approved for public release; distribution unlimited.

17. DISTRIBUTION STATEMENT (of the abstract entered in Block 20, if different from Report)

Technical note Jul 74 - aug 76,

18. SUPPLEMENTARY NOTES

19. KEY WORDS (Continue on reverse side if necessary and identify by block number)

Immittance, electromagnetic coupling, high frequency injection.

20. ABSTRACT (Continue on reverse side if necessary and identify by block number)

High frequency injection and electromagnetic coupling techniques are developed for measuring the transfer immittance of a power element. Techniques for producing artificial open and short circuits, which allows testing of power elements while in normal operation on-line, are described. An example is provided, giving the instrumentation and procedures for determining the transfer immittances of a two-port network.

DD FORM 1473 1 JAN 73   EDITION OF 1 NOV 65 IS OBSOLETE

High frequency injection and electromagnetic coupling techniques are developed for
measuring the transfer immittance of a power element. Techniques for producing artificial open
and short circuits, which allows testing of power elements while in normal operation on-line,
are described. An example is provided, giving the instrumentation and procedures for deter-
mining the transfer immittances of a two-port network.

CONTENTS

INTRODUCTION

An electrical power system is composed of various power distributing elements and loads. The properties of these elements are generally specified by the manufacturer for 60 Hz, using such standard measurements as open-circuit and short-circuit tests. Thus, if the power elements were in operation, to test them would be impossible without affecting the loads on the system because the loads must be disconnected before open- or short-circuit tests can be performed. For power elements found extensively in power distribution systems at Naval facilities, it would be advantageous to perform tests and measurements while the elements were in operation.

This report introduces a new technique to circumvent the current problems of performing tests on these elements. The new measurement technique provides the characteristic immittances, the impedances or admittances, of the power element for high frequencies (in the range from 1 kHz to 100 kHz), measured with artificial short and open circuits. These measurements can then be extrapolated down to 60 Hz to provide the operating characteristics of the power element. Perhaps the most significant facet of this new measurement technique, however, is that the element can be tested on-line in normal operation at 60 Hz. This provides the advantage of running tests without taking equipment or loads off-line and thereby minimizes equipment down time for periodic maintenance. In addition, measurements are achieved through electromagnetic coupling to minimize the effect of measuring equipment on the operation of loads.

This report, being the first on this topic, covers the theory and implementation of the measurement technique. Various theorized configurations are presented, as well as the problems and shortcomings of each. The final implementation of the method is presented in measurements carried out on a two-port network (a transformer).

1

CHARACTERIZATION OF POWER ELEMENTS

A power element is said to be characterized if its response to any given excitation can be predicted. If the element is linear, then its characteristics are described by the matrix equation:

$$[V] = [Z][I] \tag{1}$$

or

$$[I] = [Y][V] \tag{2}$$

where $[Z]$ is the impedance matrix and $[Y]$ is the admittance matrix. The general expression for the elements in the impedance matrix is:

$$Z_{ij} = \left. \frac{V_i}{I_j} \right|_{\substack{I_k = 0 \\ \text{all } k \\ k \neq j}} \tag{3}$$

The expression for the elements in the admittance matrix is:

$$Y_{ij} = \left. \frac{I_i}{V_j} \right|_{\substack{V_k = 0 \\ \text{all } k \\ k \neq j}} \tag{4}$$

The impedances Z_{ij} are measured with various currents set to zero, which implies open circuits. Thus the z-parameters are referred to as the open circuit parameters. The admittances Y_{ij}, on the other hand, are measured with various voltages set to zero, which implies short circuits, and are called the short-circuit parameters. Then, by performing open- and short-circuit tests, we can determine either the impedance or admittance parameters of the power element. Both the impedance and admittance

2

are not required, however, to characterize the power element because, if one is known, the other can be calculated. Since

$$[V] \quad = \quad [Z][I]$$

and

$$[I] \quad = \quad [Y][V]$$

then

$$[V] \quad = \quad [Z][Y][V]$$

Thus, the product $[Z][Y]$ must give the identity matrix, or that

$$[Z] \quad = \quad [Y]^{-1} \tag{5}$$

$$[Y] \quad = \quad [Z]^{-1} \tag{6}$$

If either $[Z]$ or $[Y]$ can be determined, then the element's response for any known excitation can be calculated.

For a linear element, the superposition theorem states that the total response to a number of sources is equal to the sum of the responses of each source. If the element is excited by a 60-Hz signal and a high frequency signal then

$$
\begin{array}{ccll}
[V] & = & [V_{60\,Hz}] & + & [V_h] \\
\text{total} & & \text{response} & & \text{response} \\
\text{response} & & \text{to 60 Hz} & & \text{to high} \\
& & \text{only} & & \text{frequency} \\
& & & & \text{only} \\
\\
& = & [Z][I_{60\,Hz}] & + & [Z][I_h] \\
& & \text{response to} & & \text{response} \\
& & \text{60 Hz only} & & \text{to high} \\
& & & & \text{frequency} \\
& & & & \text{only}
\end{array}
\tag{7}
$$

3

since $[V_h] = [Z][I_h]$; the element can be characterized (that is, the impedance can be determined) by measurement of the high frequency signal only. A similar derivation can be used to show that $[I_h] = [Y][V_h]$; again only high frequency measurements are required to define the admittances. Thus, if open or short circuits can be simulated for high frequency signals, and the high frequency voltage and current measured, then the z- or y-parameters can be measured with no effect on the 60-Hz AC power.

ARTIFICIAL SHORT AND OPEN CIRCUITS

A technique for producing an artificial short or open circuit (that is, one that appears like a short or open circuit to a high frequency signal but one that has no effect on the 60-Hz AC power) is introduced.

The circuit used to produce an artificial open circuit is shown in Figure 1 for a two-port network. The method, however, can be generalized for three or more port networks. The high frequency signals are injected simultaneously into both ports. The phase and amplitudes are carefully adjusted to obtain a minimum in the reading for the high frequency component of I_2, I_{h_2} (subscript h is to designate high frequency components). With I_{h_2} approximately zero, we have an open circuit in the secondary for the high frequency but not for the 60 Hz as the 60 Hz component of I_2 is not affected. Now measurements of the high frequency signals of V_{h_1}, V_{h_2}, and I_{h_1} will provide the values for Z_{11} and Z_{21}, as

$$Z_{11} = \left. \frac{V_{h_1}}{I_{h_1}} \right|_{I_{h_2} = 0} \tag{8}$$

$$Z_{21} = \left. \frac{V_{h_2}}{I_{h_1}} \right|_{I_{h_2} = 0} \tag{9}$$

In a similar fashion obtaining a minimum in the high frequency component of I_1 will provide the values of Z_{12} and Z_{22}.

Alternate proposals for producing an artificial open circuit are shown in Figure 2. A variable capacitor can be connected across the transformer terminals, as shown in Figure 2a, to form a tank circuit which is resonant at a particular high frequency. At resonance the tank circuit would appear like an open circuit. The capacitance can be adjusted to provide resonance (and thereby open circuits) at various high frequencies with no effect on the 60 Hz power signal.

The circuit in Figure 2b operates on the same principle as the one in 2a. A clamp-on device with a shunt capacitance provides the resonant circuit. Designed for resonance at high frequencies, the circuit presents a large impedance providing the artificial open circuit. The variable capacitance as before provides the capability of achieving open circuits at various high frequencies.

The circuit for producing an artificial short circuit is illustrated in Figure 3. The high frequency signals are again injected into both ports. The phase and amplitudes of the high frequency signals are adjusted to obtain a minimum in I_{hC_2}. As I_{hC_2} approaches zero, V_{h_2} approaches zero; that is, the secondary port appears like a short circuit for the high frequency signal. Measurement of V_{h_1}, I_{h_1}, and I_{h_2} will give the values of Y_{11} and Y_{21} as

$$Y_{11} = \left. \frac{I_{h_1}}{V_{h_1}} \right|_{V_{h_2} = 0} \tag{10}$$

$$Y_{21} = \left. \frac{I_{h_2}}{V_{h_1}} \right|_{V_{h_2} = 0} \tag{11}$$

5

The procedure can be repeated to obtain a minimum in I_{hC_1}, and the values of Y_{12} and Y_{22} can be determined in a similar manner.

Thus, it is possible to determine the immittance (impedance or admittance) of a power element through measurement of high frequency signals without affecting the 60-Hz signal.

ELECTROMAGNETIC COUPLING TECHNIQUES

To minimize the effects of the measuring equipment on the load, and to minimize the number of connections to the power system, the measurement of all currents will be accomplished through electromagnetic coupling. An example of the electromagnetic coupling method is illustrated in Figure 4. Through electromagnetic induction, the amplitude of the detected voltage V_o will be dependent on the magnitude of I_1. Thus, by accurately calibrating the transfer function of the ferromagnetic core $Y_T(\omega)$, we can determine the current flow from measurements of frequency and voltage V_o.

Two methods are proposed for measuring the voltage. One method is to use measurement of the amplitude of the injected high frequency signal to determine the voltage. The second method utilizes shunt reactances and electromagnetic coupling to calculate the voltage. These methods will be discussed in more detail in the "Instrumentation" section under the topic "Voltage Measurement." In most of these measurements, direct electrical connections to the power system have been eliminated because we need only measure the small high frequency signals and not the much larger 60-Hz signals. Thus, these methods provide greater safety to operating personnel as well as minimize effects of the measuring devices on the power system or loads.

The same configuration (Figure 4) can be also used to induce or inject a high frequency signal into the power system. With a high frequency source connected across the V_o terminals, a high frequency signal will be induced in the power system.

6

Two major problems were encountered in the attempts to use electromagnetic coupling to perform measurements. One was the ferromagnetic cores, which tended to saturate due to high currents found in the normal operation of power elements and resulted in nonlinear characteristics. The other significant problem was filtering out the 60 Hz and its harmonics, so that the high frequency signals could be measured.

To prevent the core from saturating, a series LC circuit was connected across the ferromagnetic core. The LC circuit was resonant at 60 Hz; it was theorized that the low impedance at resonance would shunt the 60-Hz current and thus prevent the core from saturating. At the same time, the LC circuit would present a large impedance to the high frequency signal, making detection and measurement easier. However, difficulty in obtaining resonance at precisely 60 Hz proved this scheme unsatisfactory. Also, the large capacitance required and the harmonics introduced in the system made this method impractical.

Finally, inductances were used in parallel with the cores to prevent them from saturating. The effect of these shunt inductances can be seen in Figure 5. The inductance value used in the detector circuit was picked to give a linear relationship between current I and detected voltage V_o. Thus for any given frequency, the ratio of V_o and I would be a constant value.

To minimize the effect of the 60-Hz signal, an L section filter was added, which significantly attenuated the 60-Hz signal, thereby allowing measurement of the high frequency signal.

INSTRUMENTATION

Current Measurements

The equivalent circuit of the detector circuit given in Figure 6 indicates the shunt inductance L_1 and L-section filter made up of C and L_2. The detected voltage $\overline{V}_o$ is:

7

$$\bar{V}_o = \bar{I}_2 \left(\frac{\bar{Z}_{L_1}}{\bar{Z}_{L_2} + \bar{Z}_C + \bar{Z}_{L_1}} \right) (\bar{Z}_{L_2})$$

where
$$\bar{I}_2 = \bar{I}_1/a$$
$$a = N_1/N_2 \text{ (turns ratio)}$$
$$\bar{Z}_{L_1} = j\omega L_1$$
$$\bar{Z}_C = -j/\omega C$$
$$\bar{Z}_{L_2} = j\omega L_2$$

Substituting these identities, the magnitude of V_o is:

$$V_o = \frac{I_1}{a} \left(\frac{\omega^2 L_1 L_2}{\omega(L_1+L_2) - \frac{1}{\omega C}} \right)$$

For a particular frequency, the larger the magnitude of I_1, the larger will be the magnitude of V_o. Then if the transformer core is not driven into saturation, the transfer function I_1/V_o is:

$$\left| \frac{I_1}{V_o} \right| = \frac{a \left(\omega L_1 + \omega L_2 - \frac{1}{\omega C} \right)}{\omega^2 L_1 L_2} \tag{12}$$

and presents the restriction that we cannot operate at $\omega = 1/\sqrt{C(L_1+L_2)}$. By accurately measuring the value of the transfer function I_1/V_o, we can determine the magnitude of currents from measurements of V_o and frequency. The result of calibrating the detector circuit is given in the graph of Figure 7. Illustrated are the $\left| I_1/V_o \right|$ transfer function for two different values of capacitance. Both circuits produced acceptable results; however, since the filter circuit severely attenuates signals below $f = 1/(2\pi\sqrt{(L_1+L_2)C})$, the circuit with the larger capacitance proved to be superior in providing results that could be more accurately extrapolated to obtain the parameters at 60 Hz.

8

Voltage Measurements

The method of measuring voltage using shunt capacitances and electromagnetic coupling is illustrated in Figure 8. Knowing the current, capacitance, and frequency of the high frequency signal, the voltage can be calculated from the expression:

$$V = \frac{I}{2\pi f C} \tag{13}$$

This method, employed in the experiments at CEL, provided satisfactory, duplicatable data; however, it required careful application in the measurement of z-parameters when an artificial open circuit was needed.

The other proposed voltage measurement method was developed for open-circuit testing only. The schematic diagram for the secondary terminals is given in Figure 9a. Considering only the high frequency signals, the Kirchhoff's Voltage Law equation is:

$$\bar{V}_{ind} = \bar{I}_2 \bar{Z}_{eff} + \bar{V}_2 \tag{14}$$

$\bar{Z}_{eff}$ is the impedance of the capacitor and load. With the high frequency current nulled to zero, there is an artificial open circuit and $\bar{V}_{ind} = \bar{V}_2$. A comparable circuit is shown in Figure 9b. By determining the transfer curve $A_V = V_{ind}/V_{inj}$ of the injection circuit for the high frequency range, we can theoretically determine the value of V_2 in the open circuit tests, as:

$$V_2 = V_{inj} A_V \tag{15}$$

Some serious problems, however, arose in this voltage measurement technique. The value of A_V was on the order of 10^{-3}, requiring very accurate measurements of V_{inj} to obtain reliable values of V_{ind} and V_2. Also, the value of V_2, the open-circuit voltage, could be affected by

the voltage injected in the primary side. This occurred with no discernible change in V_{inj} of the secondary. The error introduced by noise and harmonics significantly affected the measurements (so much so that this technique was considered unreliable).

The failure of the foregoing method for voltage measurement necessitated a modification of the circuit configuration for (open circuit tests) measuring z-parameters. These changes will be discussed in the section MEASUREMENT ON A TWO-PORT NETWORK.

Detector Circuit

The actual detector circuit used in the electromagnetic coupling measurements is shown in Figure 10. It consists of (1) Hewlett-Packard wave analyzer model 3581A; (2) Weston transformer coil model 327; (3) shunt inductances and filter circuit, and (4) a capacitor used for voltage measurements. The most important component in the detector circuit is item (1). It provides the high selectivity and accuracy required in the measurement of the injected high frequency voltages and currents. The wave analyzer is tunable to a particular frequency and will measure the amplitude of that particular frequency using a bandwidth as narrow as 3 Hz. Thus it filters out much of the noise, 60-Hz signal, and harmonics present on the system, providing accurate measurements on the injected high frequency signals. In addition, it is capable of accurately measuring amplitudes smaller than 0.1 microvolt, and provides a digital readout of the frequency and an analog indication of the amplitude. These features are essential to the successful characterization of the power element by electromagnetic coupling and high frequency injection techniques.

Injection Circuit

The circuitry for injecting the high frequency signal into the power element is shown in Figure 11. The circuitry consists of:

10

(1) Hewlett-Packard Audio Oscillator Model 201C (no. 2, Figure 11)

(2) Phase-shift network (no. 3, Figure 11)

(3) McIntosh MC2100 solid state stereo dual power amplifiers (no. 4, Figure 11)

(4) Weston current transformers model 327 (no. 1 and 5, Figure 11)

(5) Filter circuits and shunt inductances (no. 6 and 7, Figure 11)

The McIntosh solid state stereo power amplifier is an important part of the high frequency injection circuitry. Its two independent channels, with associated gain controls, provide the capability of simultaneously injecting high frequency signals of different amplitudes and phase into the primary and secondary sides of the transformer. The phase shift network, shown schematically in Figure 12a, provides a means of changing the phase of the high frequency signal. As the potentiometer is adjusted, the angular displacement between V_{in} and V_o is changed without affecting the magnitude of V_o. The phasor diagram in Figure 12b illustrates the phase relationship between V_{in} and V_o as the value of the resistance is changed. The controls afforded by the stereo power amplifier and phase-shift network are essential to obtaining the artificial open and short circuits required in determining the operating parameters of the power element.

In measuring the parameters of the transformer, a single audio oscillator is used to generate the high frequency signals, which insures that both signals injected into the power system have precisely the same frequency. The audio oscillator output is fed into one channel of the power amplifier and also into the phase-shift network. The signal from the phase-shift network is then fed into the other channel of the power

11

amplifier. The output of the stereo power amplifier is two signals of the same frequency, but with different amplitudes and phase, which are then injected into the primary and secondary of the transformer.

The instrumentation for measuring the parameters of the two-port network is shown in Figure 13.

MEASUREMENT ON A TWO-PORT NETWORK

z-Parameters

The initial attempt at using the electromagnetic coupling measurement techniques was carried out on a two-port network. This was a Standard Transformer, 1200V/120V, 37.5 kva, Serial No. 533604. The objective was to determine its open-circuit parameters. Several problems were encountered. Problems with the voltage measurement techniques (discussed previously in the Voltage Measurement of the INSTRUMENTATION section) necessitated modification of the circuit hookup from that indicated in Figure 1 to that shown in Figure 3, as voltage measurements would have to use shunt capacitance and electromagnetic coupling. Also, the proposed techniques of obtaining open circuits by using resonant tank circuits as illustrated in Figure 2 could no longer be used, because there was no valid method of measuring voltages with these configurations. Tank circuits also appeared to introduce harmonic interference to the system which increased the noise level, making consistent, accurate measurements difficult.

The complete detailed diagram of the instrumentation is shown in Figure 13. Using this new setup, measurement of the z-parameters were once again attempted. Great difficulty was encountered in nulling the current to obtain the artificial open circuit. With no 60-Hz AC applied, it was fairly simple to null the current to where the detected voltage V_o was a few microvolts (measured by the wave analyzer). However, with

12

60-Hz AC applied, the system harmonics and sporadic noise only allowed nulls in the range of 20 to 100 μV. These readings were often oscillating erratically; as a result, nulls were often guessed at — again making it very difficult to obtain consistent, duplicatable data.

Another problem encountered was that the currents to be measured were minuscule; and sporadic noise and harmonics played havoc with the readings. In retrospect, these very small currents could have been predicted from evaluation of the equivalent circuit of a transformer shown in Figure 14. Considering the case of an open circuit in the secondary, we have $R_L \to \infty$ and $I_2 \to 0$. The input current I_1, then, is equal to I_m, or the magnetizing current. For a typical transformer, X_ϕ and R_ϕ are very large (much larger than X_1 or R_1, respectively), which severely limits current flow in the transformer should an open circuit occur in either the primary or secondary. At high frequencies, X_ϕ would even more severely decrease the current, as its impedance is directly proportional to frequency.

These difficulties prevented the collection of any cogent data from open-circuit tests. However, as noted previously, the HP wave analyzer has the capability of measuring amplitudes less than 0.1 μV, which should be adequate for measuring the minuscule currents. To verify the validity of the artificial open-circuit test and to show that it was the harmonics and noise in the power system that prevented the achievement of reliable data, an additional experiment was conducted.

A capacitor was used in place of the two-port network, and a low pass filter was used at the input. The low pass filter would block much of the high frequency harmonics and noise of the AC power system, allowing easier detection of the injected high frequency signals. The results of the tests with 60-Hz AC applied to the capacitor correlated well with theoretically calculated values. As expected,

$$Z_{11} = Z_{12} = Z_{21} = Z_{22} = \frac{1}{\omega C}$$

13

The impracticality of using filters on all power elements, therefore, prevents using artificial open circuits in determining z-parameters. Thus z-parameter measurements were discontinued, and methods of measuring y-parameters were undertaken.

y-Parameters

The experimental setup for measuring the y-parameters is the same one as that used in the z-parameter measurements, illustrated in Figure 13. Initial indications were that the substantially larger currents would facilitate measurements of voltages and currents. The value of the shunt capacitances for voltage measurement was picked so that the detected voltage can be easily measured by the wave analyzer. Adjustments of the phase and amplitudes of the injected high frequency signals produced a distinct minimum in the measurement of V_1 or V_2. This minimum corresponds to V_1 or V_2 being approximately zero; that is, a short circuit occurs across one of the ports. These indications were very promising in view of the difficulties encountered in z-parameter measurements.

The y-parameters were first measured using conventional means. The loads were disconnected, and each port was short-circuited in turn. Measurements were made using voltmeters and ammeters. This data proved to be consistent and was used as the reference; that is, measurements using electromagnetic coupling would have to provide similar results to prove that the methods work.

Next, measurements were done using electromagnetic coupling: first without 60-Hz AC applied then with 60-Hz AC applied. The results of these measurements all correlated, as indicated by the graphs in Figure 15, which compares the results of the three tests.

The results show that $Y_{12}(j\omega)$ and $Y_{21}(j\omega)$ are approximately equal, as would be expected in a linear, reciprocal network like a transformer. $Y_{12}(j\omega)$ is 10 times larger than $Y_{11}(j\omega)$, and $Y_{22}(j\omega)$ is a hundred times larger than $Y_{11}(j\omega)$. These findings too are consistent with expected results.

14

They can be verified by the following derivations.

$$Y_{11}(j\omega) \quad = \quad \frac{I_1(j\omega)}{V_1(j\omega)}\bigg|_{V_2 = 0}$$

$$Y_{12}(j\omega) \quad = \quad \frac{I_1(j\omega)}{V_2(j\omega)}\bigg|_{V_1 = 0}$$

$$Y_{21}(j\omega) \quad = \quad \frac{I_2(j\omega)}{V_1(j\omega)}\bigg|_{V_2 = 0}$$

$$Y_{22}(j\omega) \quad = \quad \frac{I_2(j\omega)}{V_2(j\omega)}\bigg|_{V_1 = 0}$$

Also, $V_1 = aV_2$, $I_1 = I_2/a$, and $a = N_1/N_2 = 10$ for the transformer being evaluated. Then

$$Y_{12}(j\omega) \quad = \quad \frac{I_1(j\omega)}{V_2(j\omega)} \quad = \quad \frac{I_2(j\omega)}{aV_2(j\omega)} \quad = \quad \frac{I_2(j\omega)}{V_1(j\omega)} \quad = \quad Y_{21}(j\omega)$$

and

$$Y_{12}(j\omega) \quad = \quad \frac{I_1(j\omega)}{V_2(j\omega)} \quad = \quad \frac{I_1(j\omega)}{\frac{V_1}{a}(j\omega)} \quad = \quad a\left[\frac{I_1(j\omega)}{V_1(j\omega)}\right] \quad = \quad 10\,Y_{11}(j\omega)$$

and

$$Y_{22}(j\omega) \quad = \quad \frac{I_2(j\omega)}{V_2(j\omega)} \quad = \quad \frac{aI_1(j\omega)}{\frac{V_1(j\omega)}{a}} \quad = \quad a^2\left[\frac{I_1(j\omega)}{V_1(j\omega)}\right] \quad = \quad 100\,Y_{11}(j\omega)$$

15

The admittances are plotted on log-log paper in Figure 16. This result seems to indicate a purely inductive circuit. This result is not surprising if we consider the equivalent circuit for the transformer in Figure 14 under short-circuit load conditions; that is, $R_L = 0$. The circuit is simplified by considering the following conditions. In general, R_ϕ is much greater than $a^2 R_2$ and X_ϕ is much greater than $a^2 X_2$. Ignoring R_ϕ and X_ϕ then, gives a series R L circuit, with $(R_1 + a^2 R_2)$ as the resistance, and $(X_1 + a^2 X_2)$ as the total reactance. For a transformer, we expect

$$\left| (X_1 + a^2 X_2) \right| \ggg \left| (R_1 + a^2 R_2) \right|$$

so the transformer would appear like a pure inductance in the short-circuit tests. This hypothesis is borne out by the data of short-circuit tests and by the y-parameters plotted in Figure 16. The data also indicate that the approximation of the transformer as a pure inductance is valid even at 60 Hz. The results in the high frequency range can then be extrapolated to give the results for operation at 60 Hz.

The impedance parameters can be calculated from the y-parameters. For a two-port network, Equation 5 can be written

$$Z = Y^{-1} = \frac{\begin{bmatrix} y_{22} & -y_{21} \\ -y_{12} & y_{11} \end{bmatrix}}{\begin{bmatrix} y_{11} & y_{12} \\ y_{21} & y_{22} \end{bmatrix}} = \frac{\begin{bmatrix} y_{22} & -y_{21} \\ -y_{12} & y_{11} \end{bmatrix}}{y_{11}y_{22} - y_{12}y_{21}} \qquad (16)$$

$$z_{11} = \frac{y_{22}}{y_{11}y_{22} - y_{12}y_{21}} \qquad (17)$$

$$z_{12} = \frac{-y_{21}}{y_{11}y_{22} - y_{12}y_{21}} \qquad (18)$$

16

$$z_{21} = \frac{-y_{12}}{y_{11}y_{22} - y_{12}y_{21}} \tag{19}$$

$$z_{22} = \frac{y_{11}}{y_{11}y_{22} - y_{12}y_{21}} \tag{20}$$

CONCLUSIONS

In the electromagnetic coupling measurements performed by CEL, solid ferromagnetic transformer cores were used. This proved to be satisfactory for laboratory use but would not be practical for field use because power lines would have to be disconnected to pass them through the cores. For field operations, clamp-on devices such as those shown in Figure 17 could be used. This would allow setup of the measurement instruments without de-energizing the power element.

Electromagnetic-coupling measurement techniques and high frequency injection can be used to determine the circuit parameters of a power element while it is operating on-line at 60 Hz. This provides the tremendous advantage of minimizing the equipment downtime for periodic maintenance, by allowing such standard tests as open- and short-circuit tests to be run without disrupting the power supply or loads.

The techniques described in the measurement on a two-port network can be generalized to any multiport network. Thus, measurements need not be restricted to single power elements, and entire electrical systems may be measured and characterized.

After the impedances or admittances of a network have been characterized, a linear mathematical model may be synthesized. This model can then be used on an analog computer to simulate responses and operation of the network. In this manner, entire electrical power systems can be simulated and analyzed for effects of load or system changes or for responses to transients.

This method of measuring can readily be adapted for continuous monitoring of power elements or systems. Since there is essentially no effect on the system or loads, circuit parameters can be monitored continuously to provide immediate indication of faults in the power elements.

BIBLIOGRAPHY

E. A. Guillemin. Synthesis of passive networks. New York, NY, John Wiley & Sons, Inc., 1957, Chapter 6.

M. E. Van Valkenburg. Introduction to modern network synthesis. New York, NY, John Wiley & Sons, Inc., 1960, Chapter 1.

Massachusetts Institute of Technology. Magnetic circuits and transformers. New York, NY, John Wiley & Sons, Inc., 1943, Chapter 13.

D. F. Tuttle, Jr. Network synthesis. New York, NY, John Wiley & Sons, Inc., 1958, Chapter 2.

F. Kuo. Network Analysis and Synthesis. New York, NY, John Wiley & Sons, Inc., 1962, Chapter 9.

V. Del Toro. Electromechanical devices for energy conversion and control systems. Englewood Cliffs, NJ, Prentice-Hall, Inc., 1968, pp 69-84.
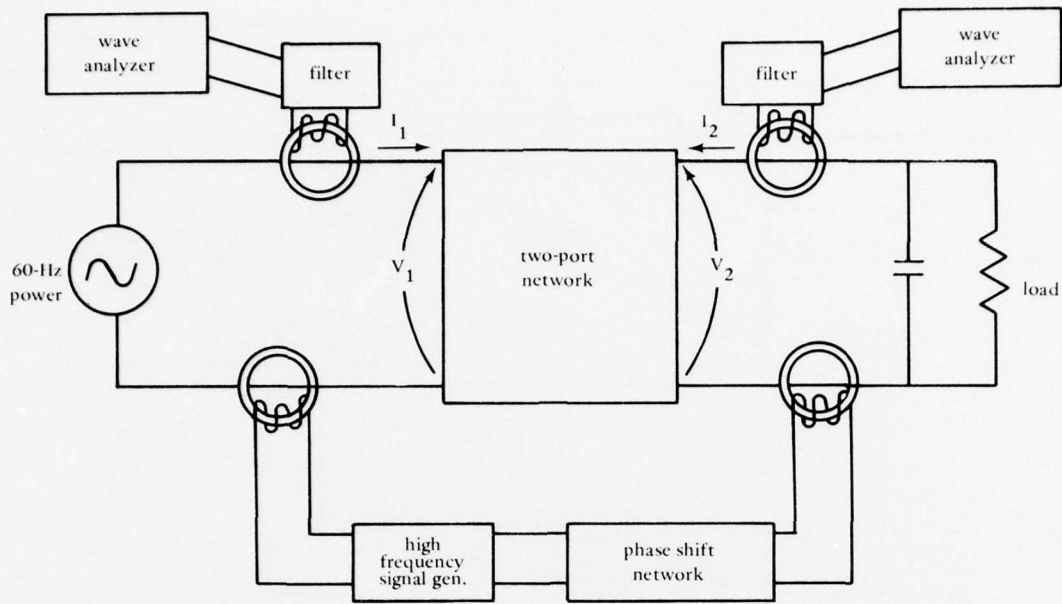
Figure 1.   Simplified circuit diagram for open–circuit simulation.

(a) Resonant tank circuit
    using shunt capacitance.

(b) Clamp-on resonant circuit.
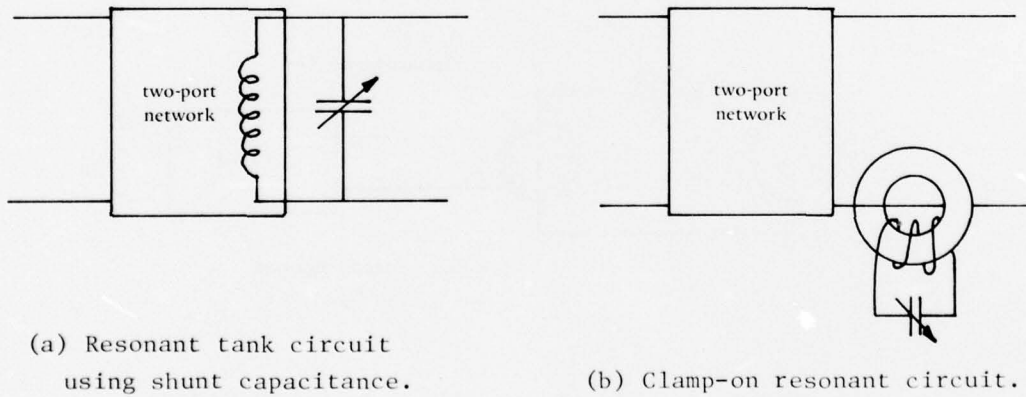
Figure 2.   Simulated open circuits using resonant circuits.

19
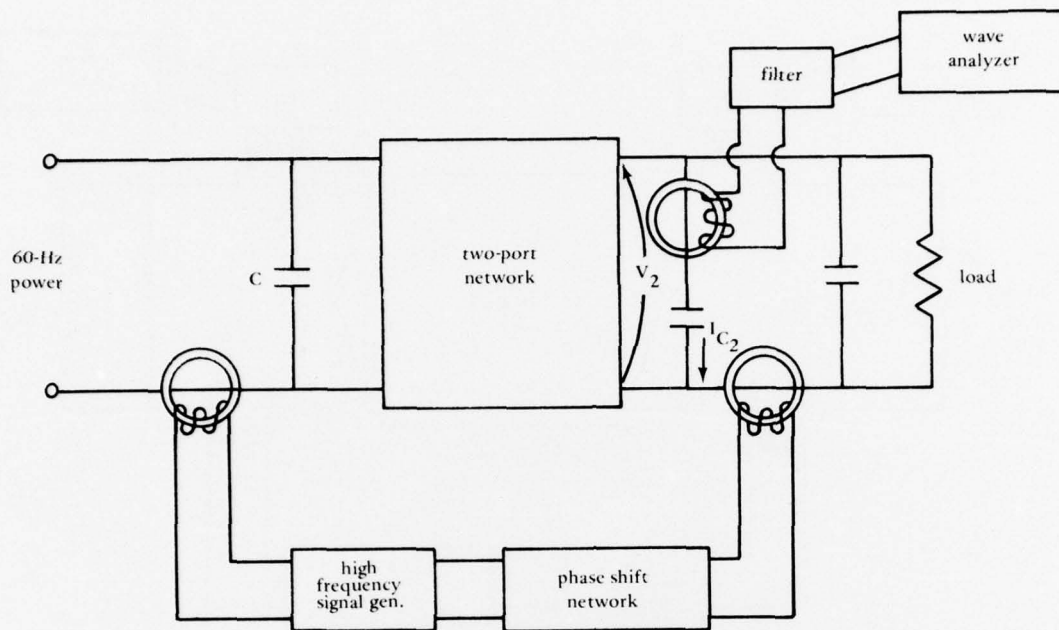
Figure 3. Simplified circuit diagram for short-circuit simulation.

$Y_T(\omega)$ = transfer function
$I_1 = Y_T V_o$
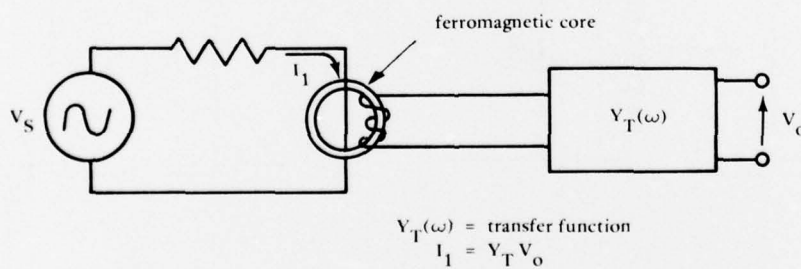
Figure 4. Electromagnetic coupling technique.

20
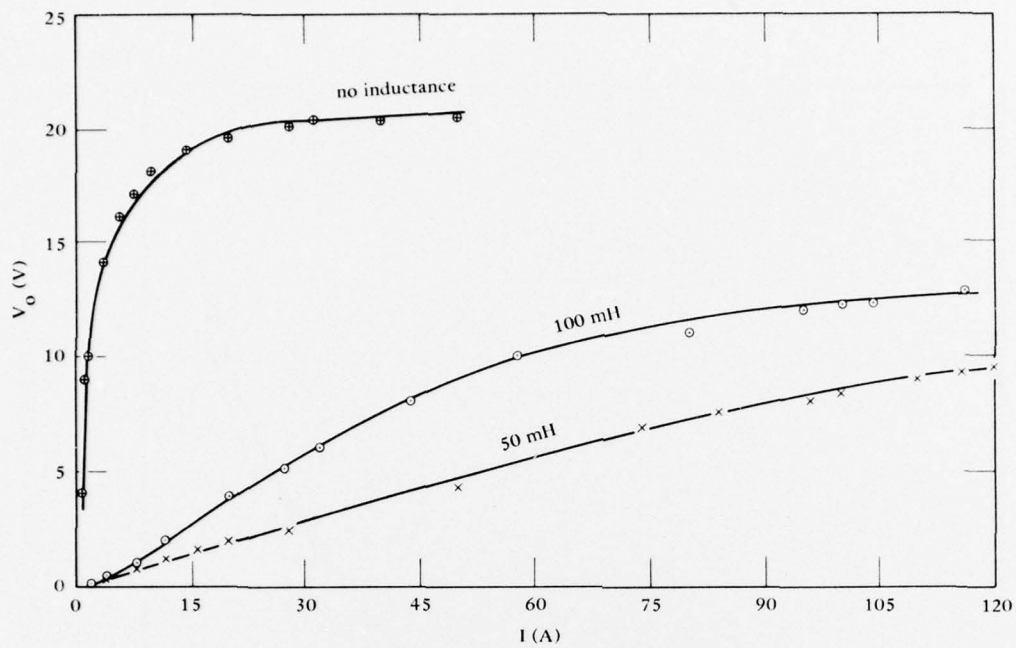
Figure 5. Effects of shunt inductance on V-I characteristics.
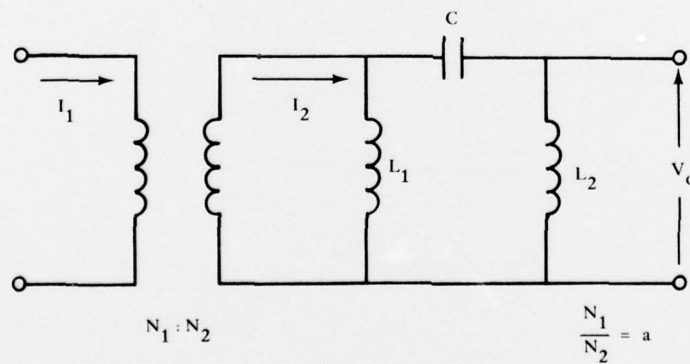
Figure 6. Schematic of ferromagnetic core and filter circuit.

21
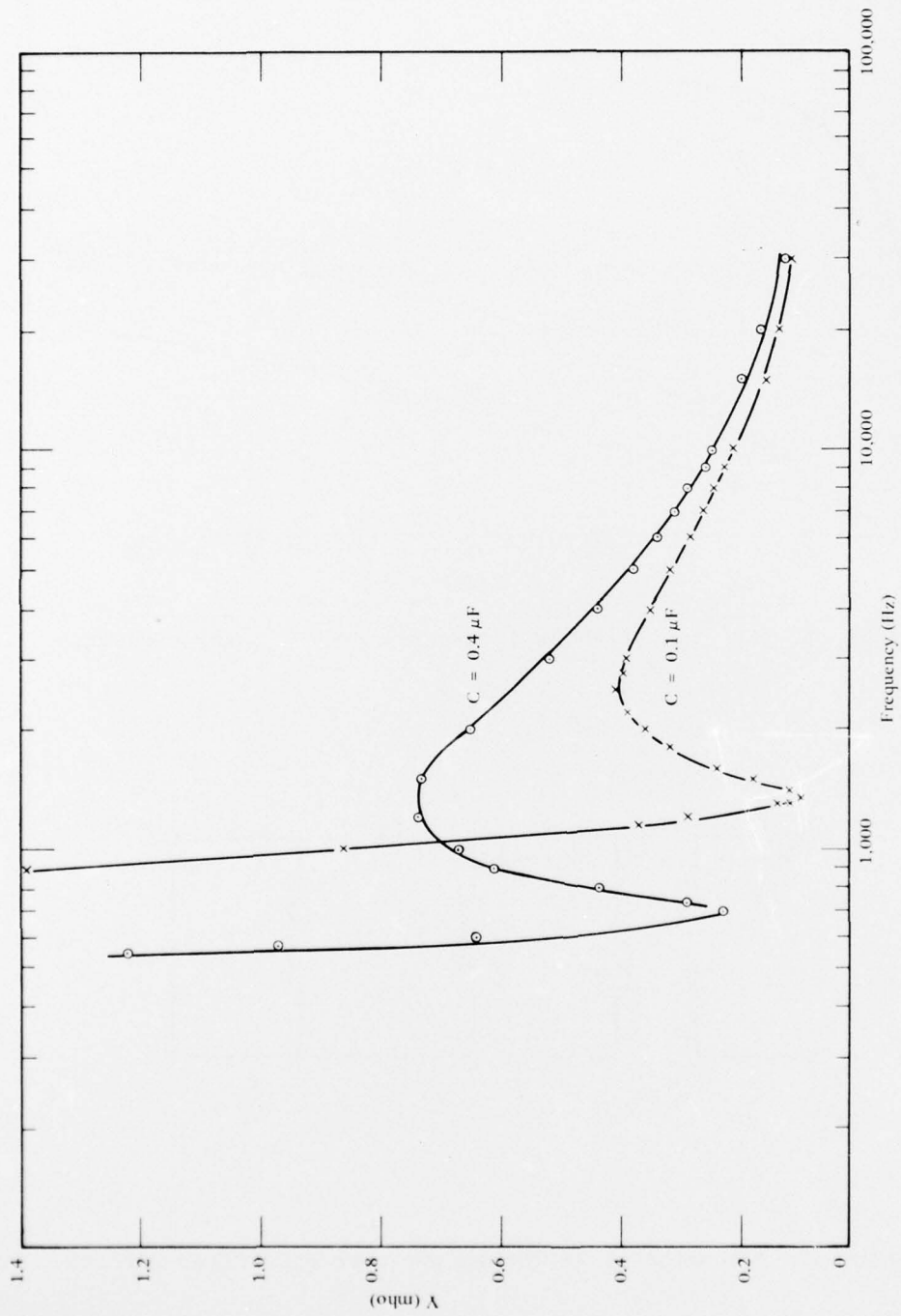
Figure 7.   Transfer curve I/V versus frequency for ferromagnetic core.

22
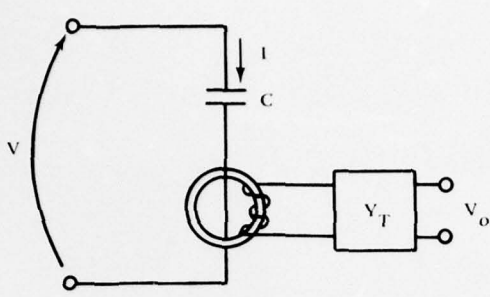
$$V = \frac{1}{\omega C}$$

$$= \frac{V_o Y_T}{2 \pi f C}$$

Figure 8. Voltage measurement with shunt capacitance.
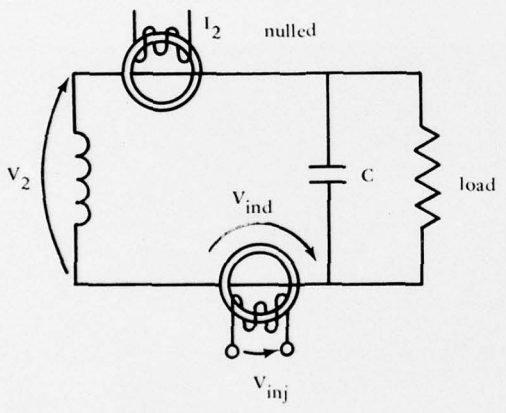
(a) Open-circuit testing.
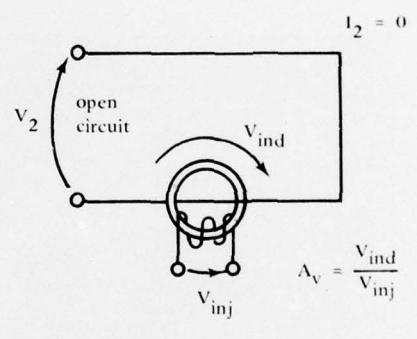
(b) Equivalent circuit for determining transfer function A_v.

$$A_v = \frac{V_{ind}}{V_{inj}}$$

Figure 9. Schematic of equivalent circuit for open-circuit testing.
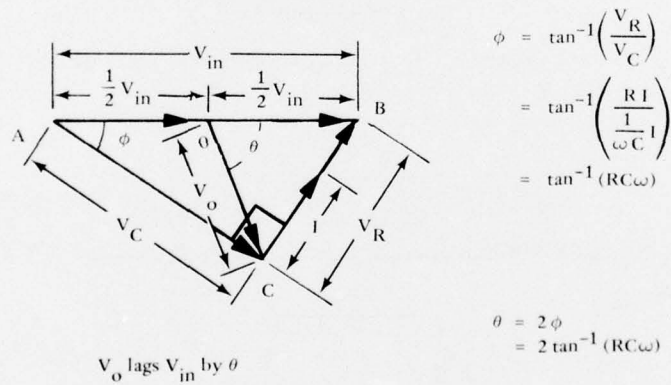
23
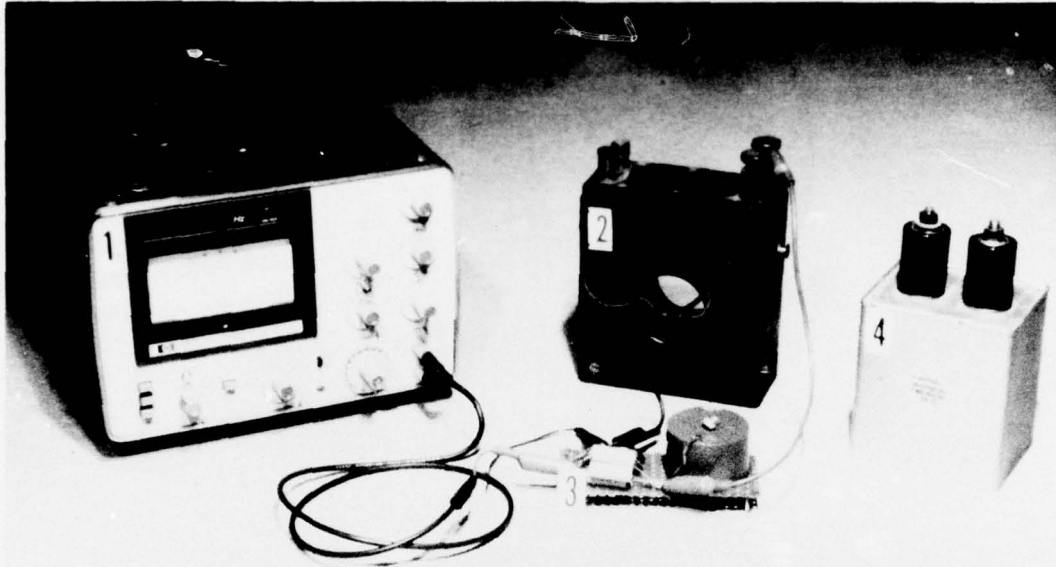
Figure 10.   Detector circuit.
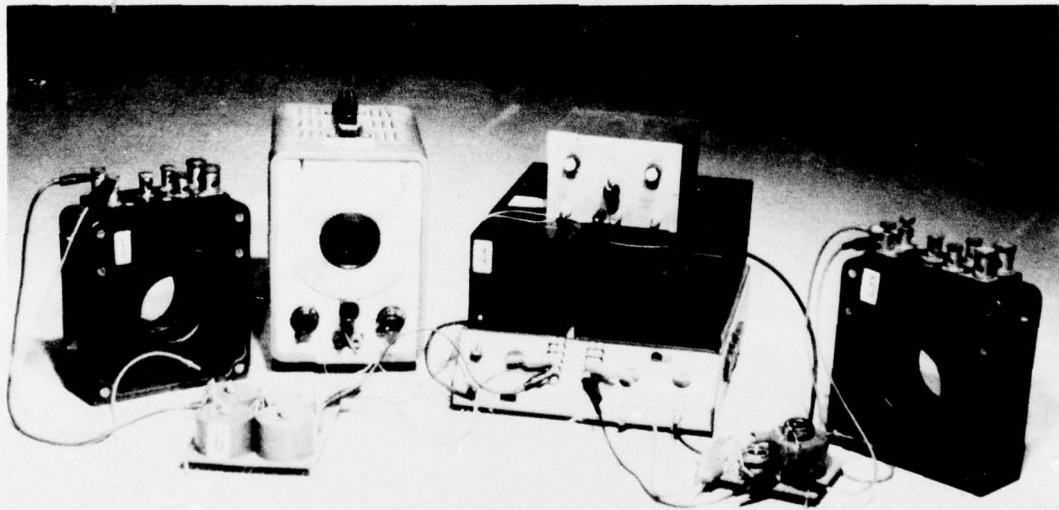
Figure 11.   Injection circuit.

$$\overline{V}_{R_1} = \overline{V}_{R_2} = \frac{\overline{V}_{in}}{2}$$

$$\overline{V}_{in} = \overline{V}_R + \overline{V}_C$$

$$\overline{V}_o = \overline{V}_C - \overline{V}_{R_2}$$

$$\overline{V}_o = \overline{V}_{R_1} - \overline{V}_R$$
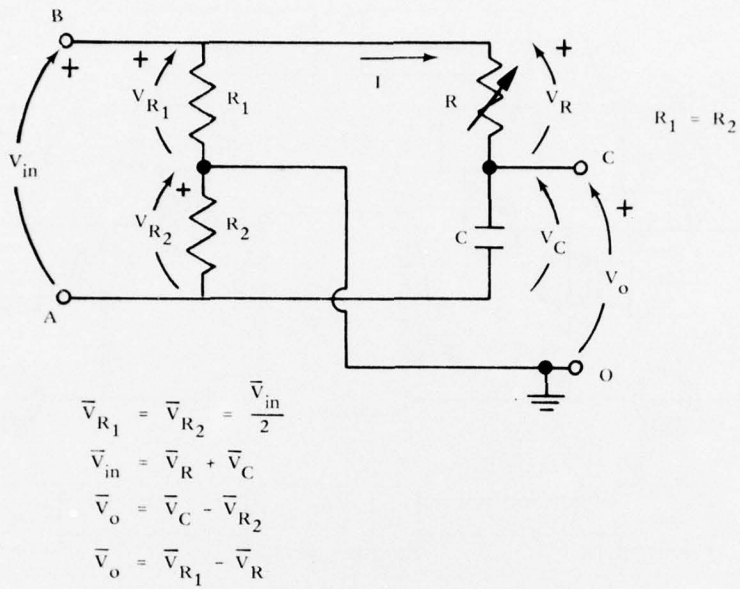
(a) Phase-shift network and voltage relationships.

$$\phi = \tan^{-1}\left(\frac{V_R}{V_C}\right)$$

$$= \tan^{-1}\left(\frac{R\,I}{\frac{1}{\omega C}\,I}\right)$$

$$= \tan^{-1}(RC\omega)$$

$$\theta = 2\phi$$
$$= 2\tan^{-1}(RC\omega)$$

V_o lags V_{in} by θ

(b) Phasor diagram showing relationship of V_{in} and V_o for some value of R.
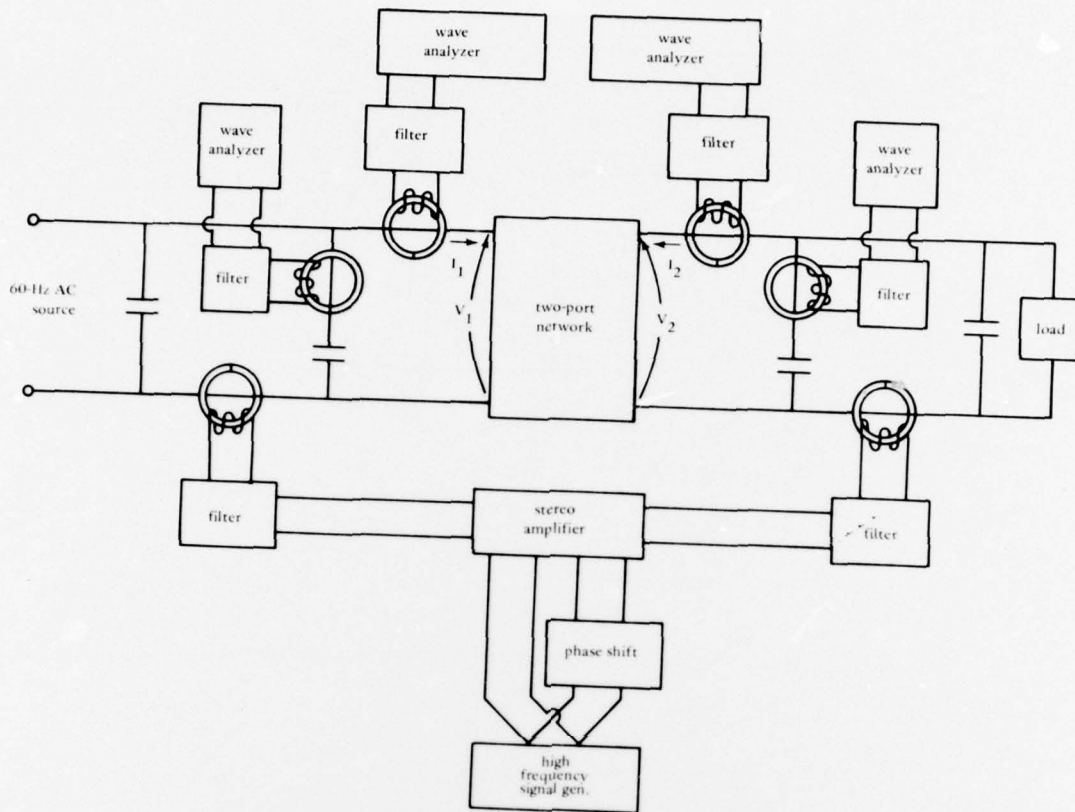
Figure 12. Phase-shift network.

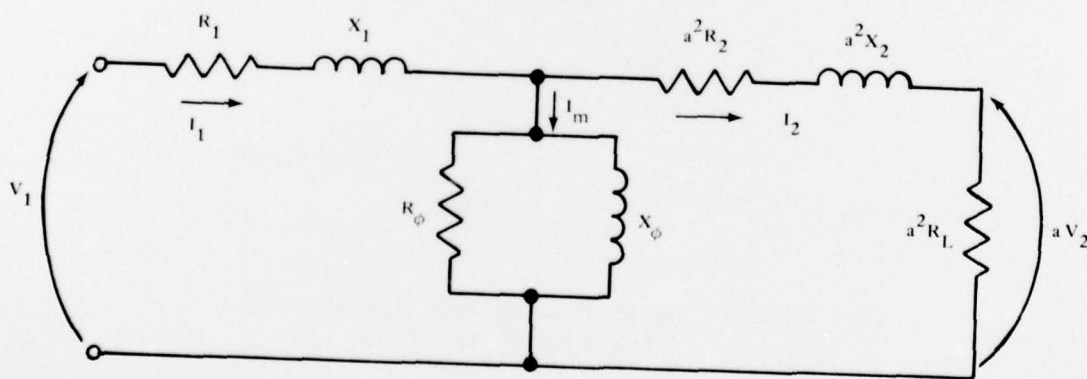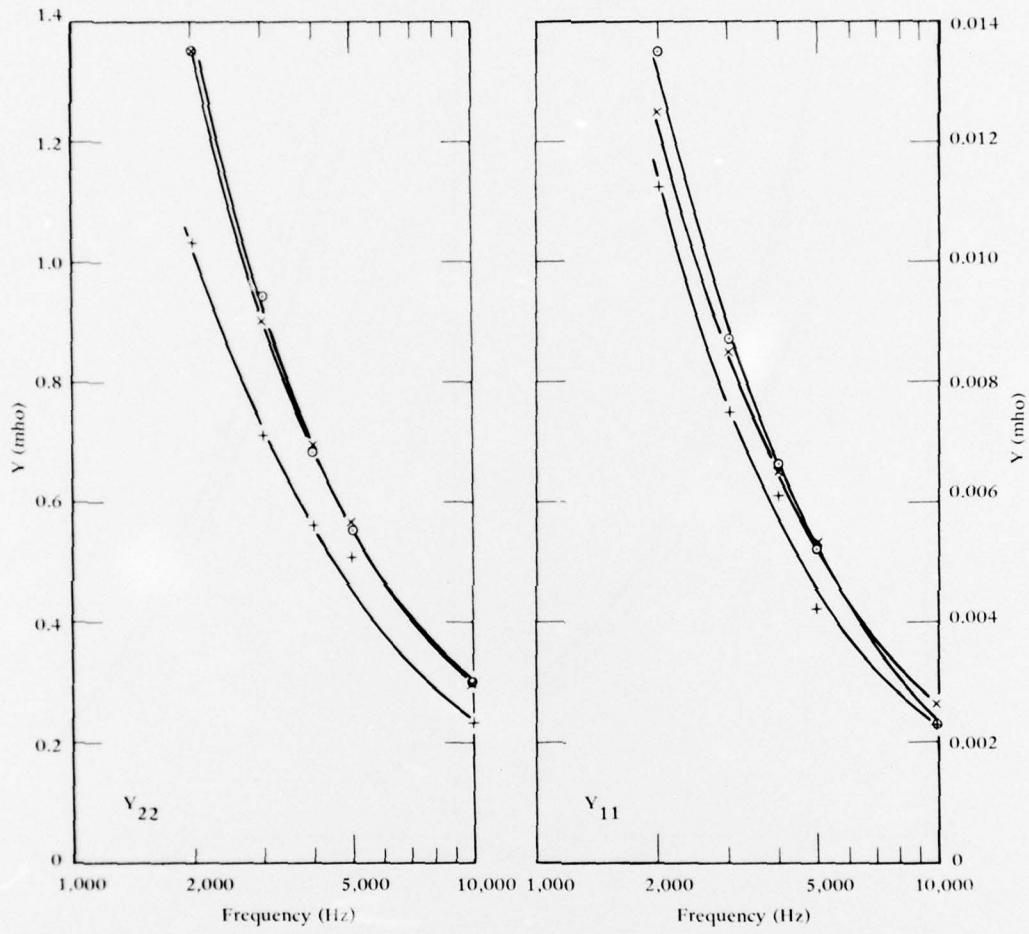Figure 13.   Instrumentation of complete circuit diagram.

Figure 14.   Equivalent circuit of transformer.

26

X Conventional measurements
O Electromagnetic coupling without 60 Hz
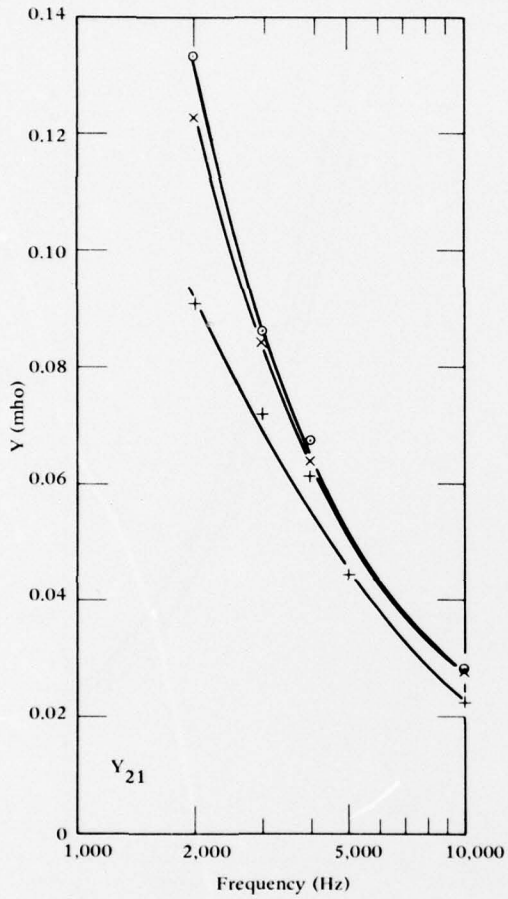+ Electromagnetic coupling with 60 Hz

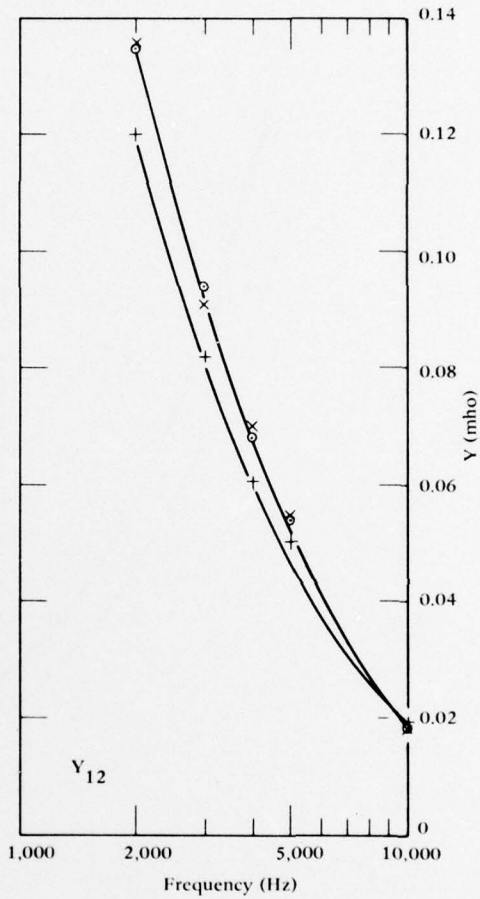(a) Y_{22} versus frequency using different measurement methods.

(b) Y_{11} versus frequency.

Figure 15.   Admittance versus frequency.

27

× Conventional measurements
⊙ Electromagnetic coupling without 60 Hz
+ Electromagnetic coupling with 60 Hz

(c) Y_{21} versus frequency.   (d) Y_{12} versus frequency.
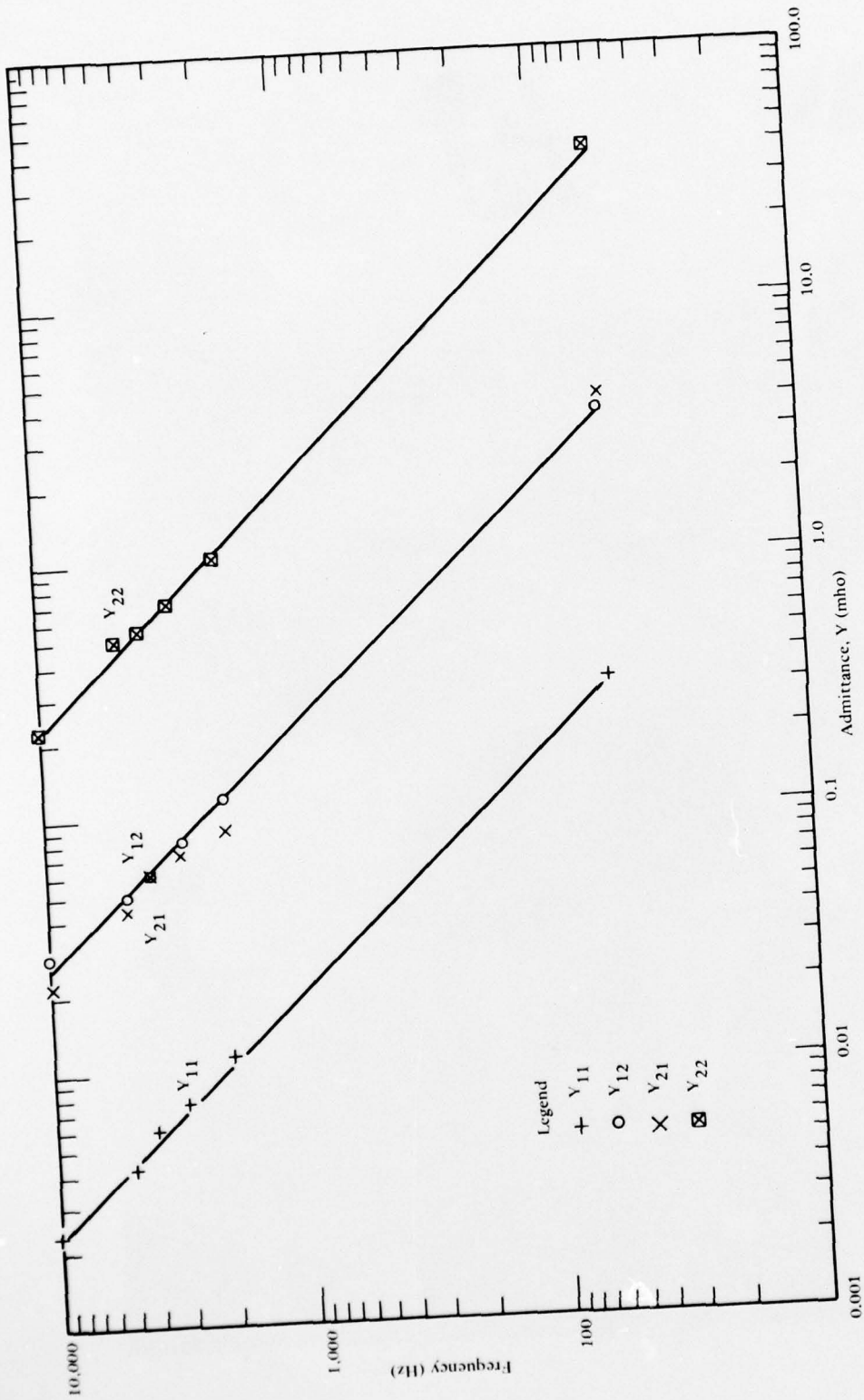
Figure 15. continued
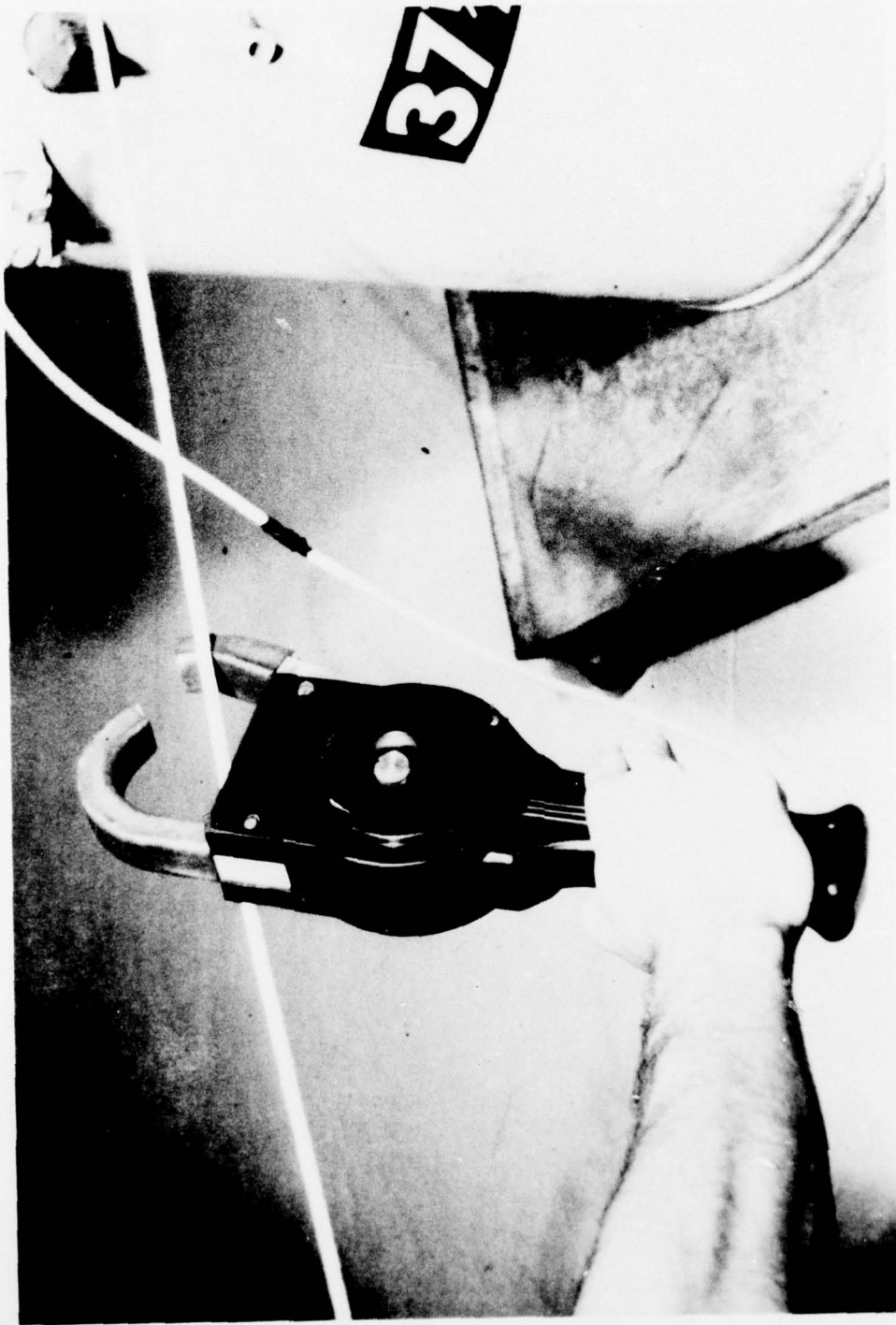
28

Figure 16. Log-log plot of Y versus frequency.

Figure 17. Clamp-on type ferromagnetic core.

DISTRIBUTION LIST

AFB AFCEC/Tech. Lib./Stop 21, Tyndall FL, AFCEC/XR,Tyndall FL, CESCH, Wright-Patterson, HQ Tactical Air Cmd (R. E. Fisher), Langley AFB VA, SAMSO/DEB, Norton AFB CA, Stinfo Library, Offutt NE

ARMY AMSEL-GG-TD, Fort Monmouth NJ, BMDSC-RC (H. McClellan, Huntsville AL, DAEN-CWE-M (LTC D Binning), Washington DC, DAEN-FEU, Washington DC, Tech. Ref. Div., Fort Huachuca, AZ

ARMY BALLISTIC RSCH LABS AMXBR-XA-LB, Aberdeen Proving Ground MD

ARMY CORPS OF ENGR Seattle Dist. Library, Seattle WA

ASST SECRETARY OF THE NAVY Spec. Assist Energy (P. Waterman), Washington DC

BUMED Code 41-1 (CDR Nichols)

BUREAU OF RECLAMATION Code 1512 (C. Selander) Denver CO

MCB ENS S.D. Keisling, Quantico VA

COMFLEACT PWO, Okinawa Japan

COMNAVMARIANAS Code N4, Guam

DEFENSE DOCUMENTATION CTR Alexandria, VA

DTNSRDC Code 42, Bethesda MD

ENERGY R&D ADMIN. Dr. Vanderryn, Washington DC

FLTCOMBATDIRSYSTRACENLANT PWO, Virginia Bch VA

KWAJALEIN MISRAN BMDSC-RKL-C

NAVFACENGCOM - LANT DIV. Eur. BR Deputy Dir, Naples Italy

MARINE CORPS BASE Code 43-260, Camp Lejeune NC, M & R Division, Camp Lejeune NC, Maint. Office, Camp Pendleton CA, PWO, Camp S. D. Butler, Kawasaki Japan

MARINE CORPS HQS Code LFF-2, Washington DC

MCAS Code PWE, Kaneohe Bay HI, Code S4, Quantica VA, PWD, Dir. Maint. Control Div., Iwakuni Japan, PWO, PWO, Yuma AS

MCB Base Maint. Offr, Quantico VA

MCRD PWO, San Diego Ca

NAD Code 011B-1, Hawthorne NV, Engr. Dir

NAS PWO., Moffett Field CA, ROICC Off (J. Sheppard), Point Mugu CA, SCE, Barbers Point HI

NATPARACHUTETESTRAN PW Engr. El Centro CA

NAVCOMMAREAMSTRSTA Code W-602, Honolulu, Wahiawa HI, PWO, Wahiawa HI

NAVCOMMSTA PWO, Adak AK

NAVFACENGCOM Code 2014 (Mr. Taam), Pearl Harbor HI

NAVREGMEDCEN SCE (LCDR B. E. Thurston), San Diego CA, SCE, Guam

NAVSCOLCECOFF C35

NAVSECGRUACT PWO, Torri Sta, Okinawa

NAVSHIPYD Code 400, Puget Sound, Code 410, Mare Is., Vallejo CA, PWO, Mare Is., PWO, Puget Sound, SCE, Pearl Harbor HI

NAVSTA PWD (L. Ross), Midway Island, PWO, SCE, San Diego CA, SCE, Subic Bay, R.P.

NAVSUPPACT CO, Seattle WA, Code 4, 12 Marine Corps Dist, Treasure Is., San Francisco CA

NAD PWD Nat./Resr. Mgr Forester, McAlester OK

NAF PWO Sigonella Sicily

NAS Asst C/S CE, Code 187, Jacksonville FL, Code 70, Atlanta, Marietta GA, Dir. Util. Div., Bermuda, PWC Code 40 (C. Kolton), PWD Maint. Div., New Orleans, Belle Chasse LA, PWD, Willow Grove PA, PWO, PWO, PWO Chase Field, PWO Whiting Fld, Milton FL, PWO, Keflavik Iceland, PWO, Kingsville TX, PWO, Millington TN, R. Kline, SCE Lant Fleet

NATNAVMEDCEN PWO

NAVAL FACILITY PWO, Cape Hatteras, Buxton NC, PWO, Centerville Bch, Ferndale CA, PWO, Guam, PWO, Lewes DE

NAVCOASTSYSLAB Code 423 (D. Good), Panama City FL, Code 710.5 (J. Quirk), Library

NAVCOMMSTA CO (61E), PWO, Balboa Canal Zone

NAVCOMMUNIT Cutler/E. Machias ME (PW Gen. For.)

NAVFACENGCOM Code 0433B, Code 0451, Code 04B3, Code 101, Code 102 (CDR Dettbarn), Code 1023 (M. Carr), Code 104

NAVFACENGCOM - PAC DIV. Code 402, RDT&E, Pearl Harbor HI, Commanders

NAVFACENGCOM - SOUTH DIV. Code 90, RDT&ELO, Charleston SC, Dir., New Orleans LA

NAVHOSP LT R. Elsbernd, Puerto Rico

NAVORDSTA PWO, Louisville KY

NAVRADRECFAC PWO, Kami Seya Japan
NAVREGMEDCEN PWO, PWO Newport RI
NAVSECGRUACT PWO, Edzell Scotland, PWO, Puerto Rico
NAVSHIPYD Code 440, Norfolk, Code 450, Charleston SC, Library, Portsmouth NH, PWO
NAVSTA CO, CO, Engr. Dir., Rota Spain, Maint. Cont. Div., Guantanamo Bay Cuba, PWO, Puerto Rico, ROICC, Rota Spain
NAVSUPPACT Maint. Div. Dir/Code 531, Rodman Canal Zone, Plan/Engr Div., Naples Italy
NAVWPNCEN PWO (Code 70), China Lake CA
NAVWPNSTA Maint. Control Dir., Yorktown VA, PWO
NAS CO, Guantanamo Bay Cuba, Code 114, Alameda CA, Code 18700, Brunswick ME, Code 18E (ENS P.J. Hickey), Corpus Christi TX, PWD (LT W.H. Rigby), Guantanamo Bay Cuba, PWD (M.B. Trewitt), Dallas TX, PWD, Maintenance Control Dir., Bermuda
NATL RESEARCH COUNCIL Naval Studies Board, Washington DC
NAVACT PWO, London UK
NAVAVIONICFAC PWD Deputy Dir. D/701, Indianapolis, IN
NAVBASE Code 111 (A. Castronovo), Philadelphia PA
NAVCOMMSTA PWO, Norfolk VA
NAVCONSTRACEN CO (CDR C.L. Neugent), Port Hueneme, CA, Code N-41, Port Hueneme CA
NAVFACENGCOM - CHES DIV, Code 101, Code 402 (R. Morony), Code 403 (H. DeVoe)
NAVFACENGCOM - LANT DIV, RDT&ELO 09P2, Norfolk VA
NAVFACENGCOM - NORTH DIV, CO, Code 1028, RDT&ELO, Philadelphia PA, Code 114 (A. Rhoads), Design Div. (R. Masino), Philadelphia PA, ROICC, Contracts, Crane IN
NAVFACENGCOM - WEST DIV, 102, 112, AROICC, Contracts, Twentynine Palms CA, AROICC, Point Mugu CA, Codes 09PA, O9P/20
NAVFACENGCOM CONTRACTS Bethesda, Design Div. (R. Lowe) Alexandria VA, Dir. Eng. Div., Exmouth, Australia, Eng Div dir, Southwest Pac, PI, OICC/ROICC, Balboa Canal Zone, ROICC, Pacific, San Bruno CA, TRIDENT (CDR J.R. Jacobsen), Bremerton WA 98310
NAVFORCARIB Commander (N42), Puerto Rico
NAVMARCORESTRANCEN ORU 1118 (Cdr D.R. Lawson), Denver CO
NAVNUPWRU MUSE DET OIC, Port Hueneme CA
NAVSCOLCECOFF CO, Code C44A
NAVSHIPYD CO Marine Barracks, Norfolk, Portsmouth VA, Code 202.4, Long Beach CA, Code 202.5 (Library) Puget Sound, Bremerton WA, Code 453 (H. Clements), Vallejo CA, Code 453 (Util. Supr), Vallejo CA, Code Portsmouth NH, PWD (Code 400), Philadelphia PA, PWD (LT N.B. Hall), Long Beach CA
NAVSTA Utilities Engr Off. (LTJG A.S. Ritchie), Rota Spain
NAVSUBASE SCE, Pearl Harbor HI
NAVSUPPACT AROICC (LT R.G. Hocker), Naples Italy, CO, Brooklyn NY
NAVTRAEQUIPCEN Technical Library, Orlando FL
NAVWPNCEN ROICC (Code 702), China Lake CA
NAVWPNSTA Code 092A (C. Fredericks) Seal Beach CA, ENS G.A. Lowry, Fallbrook CA
NAVWPNSUPPCEN PWO
NCBC CEL (CDR N.W. Petersen), Port Hueneme, CA, Code 10, PW Engrg, Gulfport MS, PWO (Code 80), PWO, Davisville RI
NCBU 411 OIC, Norfolk VA
NCBC Code 400, Gulfport MS
NCR 20, Commander
NELC Code 6700, SCE (Code 6600), San Diego CA
NMCB 5, Operations Dept., Forty, CO, THREE, Operations Off.
NROTCU Univ Colorado (LT D R Burns), Boulder CO
NSC E. Wynne, Norfolk VA
NTC Commander, SCE
OCEANSYSLANT LT A.R. Giancola, Norfolk VA
OFFICE SECRETARY OF DEFENSE OASD (I&L) Pentagon (T. Casberg), Washington DC
PMTC Pat Counsel, Point Mugu CA
PWC ENS J.E. Surash, Pearl Harbor HI, ACE Office (LTJG St. Germain), Code 116 (ENS A. Eckhart), Code 120, Oakland CA, Code 120C (A. Adams), Code 200, Great Lakes IL, Code 200, Oakland CA, Code 220, Code 505A (H. Wheeler), OIC CBU-405, San Diego CA, XO
SPCC PWO (Code 120 & 122B) Mechanicsburg PA
SUBASE NEW LONDON ENS S. Dove, Groton CT, LTJG D. W. Peck Groton CT

USCG HQ (GECV-3), Washington DC
USCG ACADEMY LT N. Stramandi, New London CT
USNA Ch. Mech. Engr. Dept, PWD Engr. Div. (C. Bradford)
WPNSTA EARLE Code 092, Colts Neck NJ
COLORADO STATE UNIV., FOOTHILL CAMPUS Engr Sci. Branch, Lib., Fort Collins CO
CORNELL UNIVERSITY Ithaca NY (Serials Dept, Engr Lib.)
DAMES & MOORE LIBRARY LOS ANGELES, CA
ENERGY R&D ADMIN. Dr. Cohen
ILLINOIS STATE GEO. SURVEY Urbana IL
LEHIGH UNIVERSITY Bethlehem PA (Linderman Lib. No.30, Flecksteiner)
LIBRARY OF CONGRESS WASHINGTON, DC (SCIENCES & TECH DIV)
MARYLAND ENERGY POLICY OFF BALTIMORE, MD (MC GUCKEN)
MASSACHUSETTS INST. OF TECHNOLOGY Cambridge MA (Rm 10-500, Tech. Reports, Engr. Lib.), Cambridge MA (Rm 14 E210, Tech. Report Lib.)
NY CITY COMMUNITY COLLEGE BROOKLYN, NY (LIBRARY)
PURDUE UNIVERSITY LAFAYETTE, IN (CE LIB)
UNIVERSITY OF CALIFORNIA BERKELEY, CA (OFF. BUS. AND FINANCE, SAUNDERS), Berkeley CA (E. Pearson)
UNIVERSITY OF DELAWARE Newark, DE (Dept of Civil Engineering, Chesson)
UNIVERSITY OF ILLINOIS URBANA, IL (LIBRARY)
UNIVERSITY OF MASSACHUSETTS (Heronemus), Amherst MA CE Dept
UNIVERSITY OF NEBRASKA-LINCOLN LINCOLN, NE (SPLETTSTOESSER)
UNIVERSITY OF TEXAS Inst. Marina Sci (Library), Port Aransas TX
UNIVERSITY OF WISCONSIN Milwaukee WI (Ctr of Great Lakes Studies)
URS RESEARCH CO. LIBRARY SAN MATEO, CA
US DEPT OF COMMERCE NOAA, Pacific Marine Center, Seattle WA
BECHTEL CORP. SAN FRANCISCO, CA (PHELPS)
DURLACH, O'NEAL, JENKINS & ASSOC. Columbia SC
MCDONNEL AIRCRAFT CO. Dept 501 (R.H. Fayman), St Louis MO
OCEAN DATA SYSTEMS, INC. SAN DIEGO, CA (SNODGRASS)
SHELL DEVELOPMENT CO. HOUSTON., TX (TELES)
WESTINGHOUSE ELECTRIC CORP. Annapolis MD (Oceanic Div Lib, Bryan)
WISS, JANNEY, ELSTNER, & ASSOC Northbrook, IL (J. Hanson)
WOODWARD-CLYDE CONSULTANTS PLYMOUTH MEETING PA (CROSS, III)
BRYANT ROSE Johnson Div. UOP, Glendora CA
T.W. MERMEL Washington DC